Non-Invasive Measurement of Brain Temperature with Microwave Radiometry: Demonstration in a Head Phantom and Clinical Case

PAUL R. STAUFFER[1,2], BRENT W. SNOW[3,4*], DARIO B. RODRIGUES[1,5], SARA SALAHI[1,6], TIAGO R. OLIVEIRA[1,7], DOUG REUDINK[4*], PAOLO F. MACCARINI[1]

[1] Departments of Radiation Oncology and Biomedical Engineering, Duke University; Durham, NC, USA
[2] Department of Radiation Oncology, Thomas Jefferson University; Philadelphia PA, USA
[3] Department of Surgery and Urology, University of Utah; Salt Lake City, UT, USA
[4] Thermimage Inc.; Salt Lake City, UT, USA
[5] CEFITEC, FCT, New University of Lisbon; Caparica, Portugal
[6] ANSYS, Inc.; Irvine, CA, USA
[7] Institute of Physics, University of São Paulo; São Paulo, Brazil

Key words: microwave radiometry, core temperature, brain temperature, non-invasive thermometry

SUMMARY – *This study characterizes the sensitivity and accuracy of a non-invasive microwave radiometric thermometer intended for monitoring body core temperature directly in brain to assist rapid recovery from hypothermia such as occurs during surgical procedures. To study this approach, a human head model was constructed with separate brain and scalp regions consisting of tissue equivalent liquids circulating at independent temperatures on either side of intact skull. This test setup provided differential surface/deep tissue temperatures for quantifying sensitivity to change in brain temperature independent of scalp and surrounding environment. A single band radiometer was calibrated and tested in a multilayer model of the human head with differential scalp and brain temperature. Following calibration of a 500MHz bandwidth microwave radiometer in the head model, feasibility of clinical monitoring was assessed in a pediatric patient during a 2-hour surgery. The results of phantom testing showed that calculated radiometric equivalent brain temperature agreed within 0.4°C of measured temperature when the brain phantom was lowered 10°C and returned to original temperature (37°C), while scalp was maintained constant over a 4.6-hour experiment. The intended clinical use of this system was demonstrated by monitoring brain temperature during surgery of a pediatric patient. Over the 2-hour surgery, the radiometrically measured brain temperature tracked within 1-2°C of rectal and nasopharynx temperatures, except during rapid cooldown and heatup periods when brain temperature deviated 2-4°C from slower responding core temperature surrogates. In summary, the radiometer demonstrated long term stability, accuracy and sensitivity sufficient for clinical monitoring of deep brain temperature during surgery.*

Introduction

Hypothermia, where body core temperature drops below 36°C, can triple the risk of morbid myocardial outcomes following surgery [1], triple the risk of surgical wound infection [2,3], increase blood loss [4-6], increase transfusion requirements [4-6], prolong surgical recovery [7], and extend the duration of hospitalization [2]. It is therefore imperative that anesthesiologists monitor and effectively manage core temperature and for rapid recovery to good health, reestablishing normothermic temperature of the internal organs is essential. Although brain is the most critical tissue [8], core temperature is usually considered to be the temperature of internal

[*] *Brent Snow and Doug Reudink are officers of Thermimage Inc.*

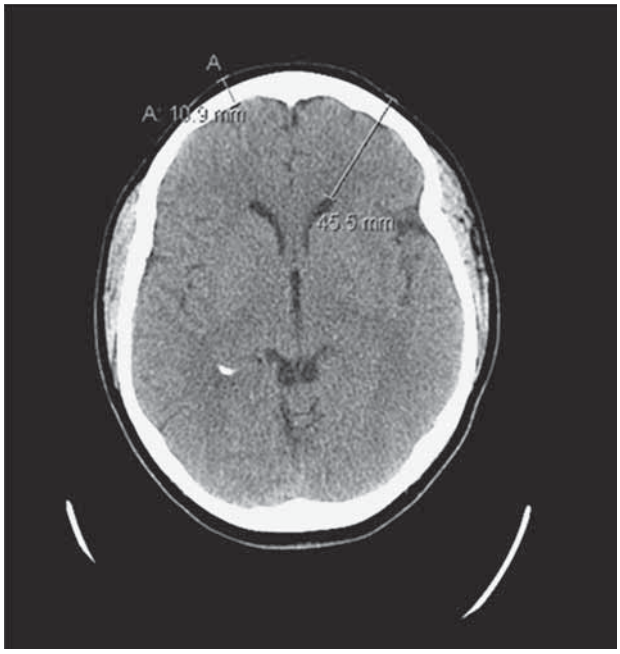

Figure 1 CT scan of a 66-year-old female head. The collective thickness of skull and scalp is 10.9 mm in the forehead region and the distance from skin to ventricle deep in brain is 45.5 mm.

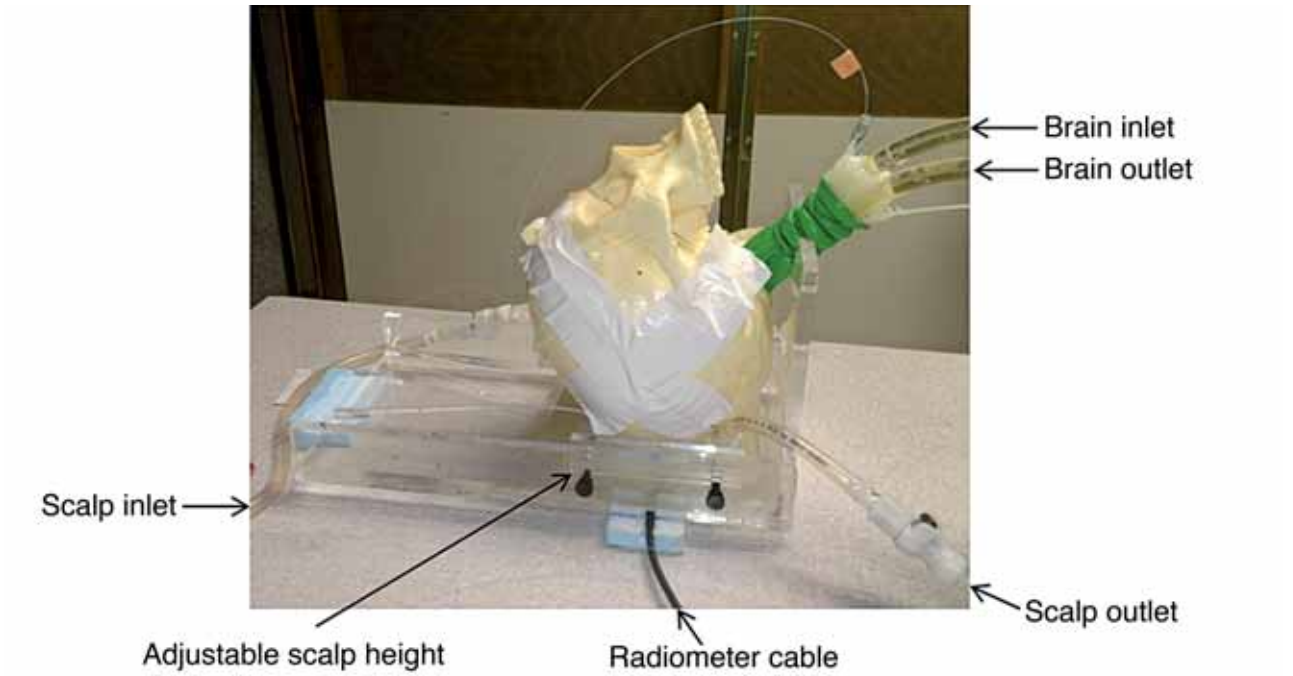

Figure 2 Human head model with variable temperature brain tissue-equivalent liquid circulating through a balloon that fills the inside of the skull, and temperature controlled scalp tissue-equivalent liquid circualting through an adjustable thickness "scalp" under the skull. The black cable connects the external radiometer readout to the front stage radiometer and antenna sensor which is coupled to the scalp through a thin mylar window and facing upwards into the skull.

body organs which can differ significantly from brain. In fact, current thermometry devices typically measure only surface temperatures or intracavitary surrogates of body temperature that do not accurately reflect core temperature of the deep lying organs, especially brain. Each of these surrogate core temperature measurements has inherent problems with probe placement, time delays in reading true core temperature, and/or are objectionably invasive [9,10].

Readily available non-invasive measurements include axillary and forehead surface thermometers which vary with contact, movement, perspiration, and environment, producing an unreliable prediction of temperature deep in the body core [11,12]. Infrared thermography can non-invasively sense thermal energy emitted from tissue close to the surface, but those measurements do not reflect temperatures deep in the body. In particular, temperature measurement of the temporal artery takes advantage of high perfusion in the region which could reflect core temperature, but calibration of such readings is highly dependent on skin emissivity, perspiration, and environment which vary greatly for typical operating room conditions [11,12]. Infrared measurements of the tympanic membrane have the potential to reflect core body temperature accurately but in clinical practice are less reliable due to the tortuous anatomy of the ear canal and presence of cerumen [11,13]. Invasive measurements of core temperature are generally accomplished either with intracavitary devices like rectal, Foley, nasopharyngeal, endotracheal and esophageal probes, or with temperature sensors placed interstitially in the pulmonary artery [11,13-15]. Placement of internal temperature probes is uncomfortable, may require sedation or anesthesia, and is not without risk. The accuracy of these invasive probes depends on many factors [11,16]. For instance, the position of nasopharyngeal temperature probes placed under anesthesia is uncertain and the amount of mouth breathing or endotracheal tube air leakage affects the readings. Rectal probes work best if the probe tip is located against the perfused rectal wall rather than inside a feces, but this is difficult to ensure and if partially insulated from the rectal wall there may be significant delays in reading surrounding body temperature. Accuracy of bladder thermometry via a Foley catheter depends on urine production, bladder volume and probe location within the bladder. Like rectal measurements, Foley probes generally exhibit significant time delays in reading actual body core temperature, especially when the temperature is changing rapidly from intentional external heating or cooling. The most invasive temperature probe is a pulmonary artery catheter which is passed through a vein into and through the right atrium of the heart into the pulmonary artery. This is currently considered to be the best core temperature measurement [13]. However, only severely ill or high-risk surgical patients warrant pulmonary artery monitoring due to the potential risks of such an invasive procedure. And because of their status, these patients often receive large amounts of room temperature IV fluids as well as refrigerated blood products that reduce the accuracy of this core temperature reading.

This investigation reports preliminary testing of a novel non-invasive core temperature thermometer that uses a small microwave radiometric sensor on the surface to measure thermal radiation emitted from tissue in the 1.1-1.6 GHz band. Unlike infrared radiation which travels less than a centimeter to the surface, thermal emissions in the microwave range travel many centimeters through tissue. The amount of microwave energy received by a surface antenna increases with increasing tissue temperature and may be used to quantify deep tissue temperature. We choose to monitor temperature inside the brain [17] rather than alternative sites due to the critical nature of this organ and its central role in thermoregulation [8,16]. The purpose of this study is to characterize the sensitivity and accuracy of a new radiometric thermometer for long-term monitoring of core temperature in brain. To demonstrate the performance of the device, we built a realistic phantom model of the human head with separate brain and scalp regions consisting of tissue equivalent liquids circulating at independent temperatures on either side of an intact skull. This life size multilayer model of the human head allows simulation of differential surface and deep tissue temperatures. Thus, the quantification of radiometer sensitivity to changes in brain temperature becomes independent of scalp and operating room temperatures.

Methods

The key innovation of this project is the integration of two critical components: a small (2.5 cm diameter) receive antenna specifically optimized with electromagnetic simulation software (HFSSTM - Ansys, Canonsburg, PA, USA) for deep penetration into the human head, and a high gain 1.1-1.6 GHz microwave radiometer with miniature printed circuit chip components mounted on the back of the antenna sensor. The radiometer circuit achieves high sensitivity and noise rejection using a dual-matched ultralow noise high gain amplifier design that maintains the receive antenna connection directly to the front stage amplifier for high sensitivity while providing a time se-

Figure 3 2.5 cm diameter tapered log spiral microstrip antenna encapsulated together with the radiometer electronics printed circuit on the back surface of antenna inside a cylindrical copper tube with 1 mm wall thickness.

quenced comparison to internal temperature reference for long-term stable calibration [18]. The entire sensor package is contained in a lightweight and low profile 2.8 cm diameter by 1.5 cm high assembly that can be held in place over the skin with an electromagnetic interference (EMI) shielding adhesive patch and/or elastic strap.

Experimental Model of Human Head

In order to test this core temperature-sensing device, a multilayer tissue phantom model of the human head was constructed. The literature reports a range of dimensions for the constituent tissues of the human head [19], with scalp consisting of skin that ranges from 3 mm (forehead) to 8 mm (occipital region) thick and subcutaneous fat and fibrous tissues from 4 mm to 7 mm thick overlying the skull. To generate a realistic physical model for radiometric measurements, a de-identified human brain CT scan dataset (e.g. Figure 1 slice) was analyzed with tissue segmentation software (Avizo, FEI Visualization Sciences Group, Burlington MA, USA) to establish appropriate values for the thickness of scalp, bone, and brain tissues. Measurements from this CT dataset showed that the scalp (skin/fat/muscle) varied from 4.2 mm (forehead) to 10 mm (temporal lobe) thick and the skull bone was 6.7 mm thick in both regions. These measurements are in general agreement with the literature [19]. The distance from the forehead surface to the ventricle deep in brain was 45.5 mm for this patient. Based on these tissue dimensions, an experimental model of the human head was constructed from tissue mimicking phantom mixtures for scalp and brain tissues that fit around an artificial human skull (Life Size Skull, www.anatomywarehouse.com) having geometry and dielectric properties similar to skull bone. A photograph of the experimental model is shown in Figure 2.

To model the thermodynamics of scalp which is a mixture of skin, fat and muscle tissues, an adjustable thickness (6-16 mm) compartment was sealed against the outer surface of the skull and filled with temperature-controlled distilled water (ε_r = 74.2, σ = 0.28 at 1.35 GHz) that was circulated at 1.7 l/min flow rate to maintain a homogeneous stable scalp temperature. To simulate brain, a mixture of ethylene glycol, water and NaCl was used to approximate the electrical properties of mixed grey and white matter (ε_r = 52.43, σ=1.45 S/m at 1.35 GHz). Dielectric properties of the phantom tissue components were characterized using a coaxial dielectric properties probe (E85070C, Agilent Technologies, Santa Rosa CA, USA) connected to a network analyzer (E5071C, Agilent Technologies) and adjusted to conform with Cole-Cole data for the respective biological tissues [20]. The liquid brain phantom was circulated vigorously (~3 l/min) with a peristaltic pump through a latex balloon that filled the interior of the skull, and temperature was controlled with a heat exchanger to mimic changes in deep brain temperature resulting from anesthesia and subsequent thermoregulatory responses. Temperatures of scalp and brain were controlled independently to provide a range of different surface: deep temperature gradients typical of various surgical procedures. These temperature gradients were used for calibration of the temperature conversion algorithm in order to distinguish volume averaged brain temperature from cooler and warmer scalp, and for subsequent testing of radiometer performance.

Radiometric Sensor

In consideration of clinical constraints for monitoring brain temperature in an operating room, the design goal was a lightweight sensor with maximum outer diameter of 2.8 cm and height of 1.5 cm that can be held in position on the scalp with adhesive and/or an elastic band. The radiometric sensor (Figure 3) consists of a thin wall copper tube enclosure containing a 2.5 cm dia microstrip antenna with a deep penetrating receive pattern and a 1.1-1.6 GHz printed circuit radiometer on the back side of the antenna to preamplify and filter the received signal for transmission through a 2 m coaxial cable to an external readout. The radiometer circuit and software that convert the received signal into a weighted volume average temperature of tissue under the antenna have been described previously [21-24]. The 2.5 cm dia thick substrate tapered log spiral microstrip antenna was optimized for temperature monitoring of deep brain through iterative design in HFSS, based on an accurate computational model of the human head phantom with dimensions determined from a CT scan of the model and dielectric properties as measured in the brain, bone, and scalp regions. The optimization parameter for the HFSS design was the ratio of electromagnetic radiation received from brain to that received from all tissue under the antenna over the 1.1-1.6 GHz band. Simulations were performed for antennas in the active mode, where energy is transmitted and consequently absorbed by the tissue underlying the antenna. This effect is quantified by the power deposition pattern, or specific absorption rate (SAR) distribution in tissue. When used for radiometric monitoring purposes, the antenna is in the passive mode where it collects energy emitted from tissue rather than transmitting energy into it. Due to reciprocity, the pattern of received energy in the passive monitoring mode is the same as that radiated in the active mode, and the same antenna optimization technique is valid for both modes. This computational method has been validated experimentally in similar antennas [21-24].

Thermal Dosimetry Experiments

An initial steady state condition was established in the head phantom by circulating 32°C scalp phantom through the bolus covering the skull surface and 37°C brain phantom through the latex balloon filling the interior of the skull. Circulation was maintained for approximately 50 min with the head at thermal equilibrium and the radiometer stable. In order to demonstrate the radiometer's ability to measure temperature from many centimeters deep in the head distinctly from surface temperature changes in the scalp, the temperature of the circulating brain phantom was abruptly decreased by 10°C while maintaining the scalp at constant 32°C for approximately 90 min. Radiometric power (P) was measured continuously and converted into equivalent temperature (T) using P=mGT, where m is a calibration constant and G is the gain calculated from the radiometric signal from the known temperature reference load. Brain temperature was varied and scalp temperature held constant. To demonstrate the accuracy and stability of radiometric readings over an extended time such as long open heart surgery, the circulating brain temperature was changed abruptly +10°C back to its original baseline (37°C) and maintained steady for an additional two hours. Temperatures of both phantom tissue regions were monitored continuously during the experiment using fiberoptic sensors (Luxtron 3100, LumaSense Technologies, Santa Clara, CA, USA) for comparison with the radiometric readings.

Error and Statistical Analyses

The radiometric signal was smoothed using a 200-400 point moving median calculation in order to eliminate the short-term fluctuations from EMI environmental noise. Radiometer accuracy was quantified in terms of measurement error, defined by the absolute difference between brain temperatures measured by the fiberoptic probe and calculated from radiometric received power. A statistical analysis of the difference was implemented for each segment of the experiment: initial steady state with 37°C brain and 32°C scalp, rapid brain cooling, steady state plateau at 27°C brain temperature, rewarming, and final steady state plateau with brain returned to 37°C. The minimum, maximum, and average +/– standard deviation (SD) of differences between radiometer and fiberoptic measured brain temperatures were calculated over each segment and for the entire experiment.

Clinical Correlation

In order to demonstrate the clinical feasibility of this radiometric monitoring approach, an Institutional Review Board approval was

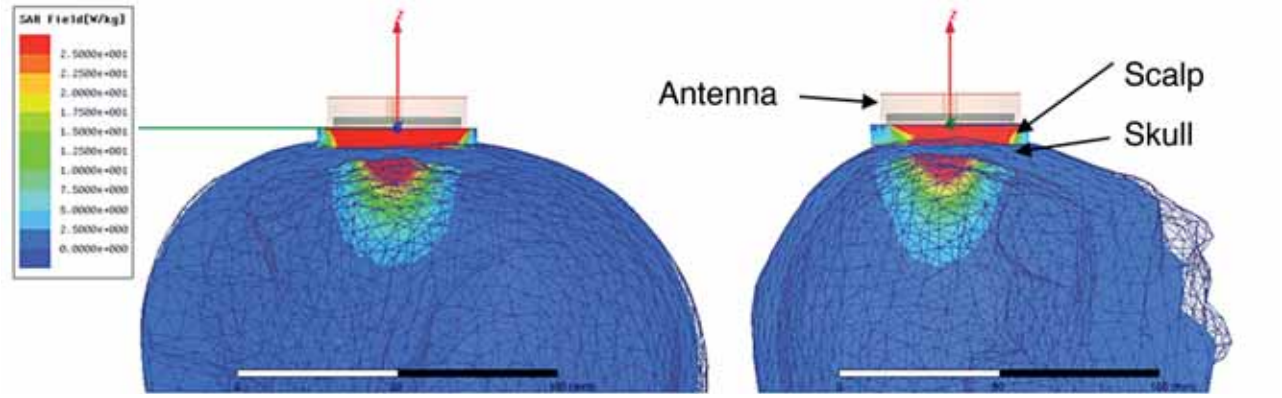

Figure 4 HFSS-simulated SAR pattern of a 2.5 cm diameter log spiral microwave antenna on the human head model. Simulations performed at the center band frequency of 1.35 GHz demonstrate that the radiometer is sensitive to scalp temperature (maximum SAR and received power in red) but receives a significant portion of the energy at 1.35 GHz from brain tissues inside the skull.

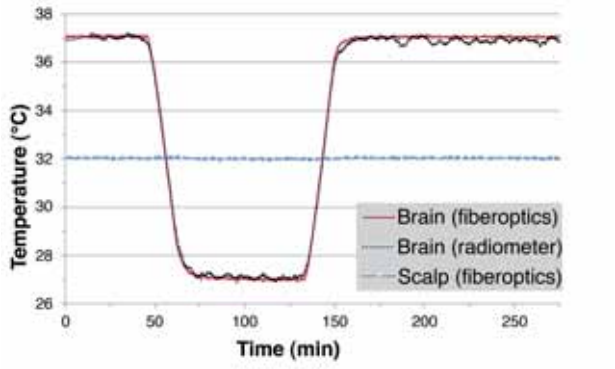

Figure 5 Equivalent brain tissue temperature (black) calculated from total power receiveed by a non-invasive radiometric sensor closely mirrors the actual temperature of the cirulating variable temperature brain phantom (red) as measured through constant temperature scalp tissue (blue), with no significant error from drift in radiometer calibration over 4.5 hours of monitoring.

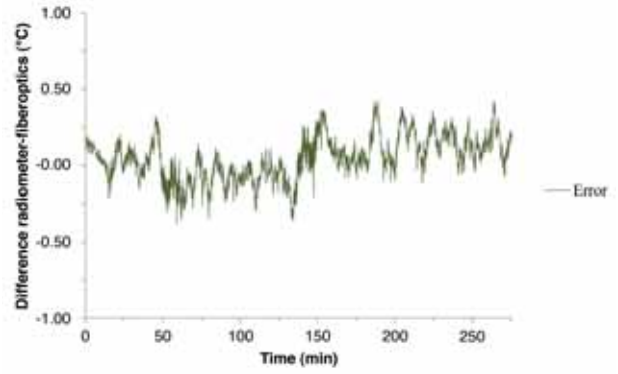

Figure 6 Absolute temperature difference between the equivalent brain temperature calculated from radiometer received power readings and the fiberoptic probe measured temperature of circulating brain phantom.

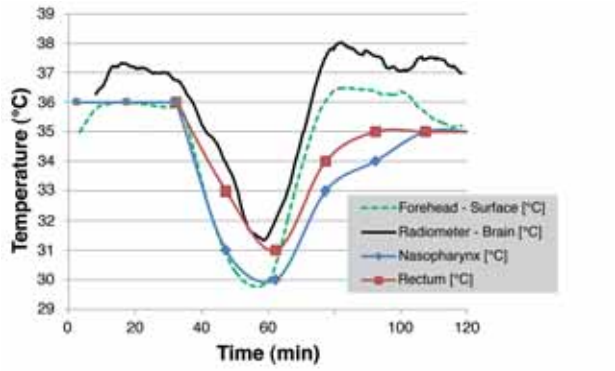

Figure 7 Equivalent brain temperature (black) from 400-point median calculations of raw radiometric readings during surgery of pediatric patient, correlated with manually recorded rectal (red) and nasopharyngeal (blue) core temperature measurements and skin surface just under the radiometric sensor (green dashed line). Note the large (up to 4°C) difference in core temperature readings during the time of rapid temperature change in the patient and closer agreement of core measurements after a period of steady state (1-2°C).

obtained for passive non-invasive monitoring of pediatric brain temperature during surgery. For initial proof of concept, a radiometric sensor was placed on the temple of a one-year-old male patient – undergoing ventriculoseptal defect repair surgery – to radiometrically measure brain temperature. As is typical in this operating room, body tempera-

Table 1 Statistical analysis of the temperature difference $T_{fiberoptic} - T_{radiometer}$ over each segment of the phantom model heating and cooling experiment.

Segment	*Time*	*Min (°C)*	*Max (°C)*	*Ave (°C)*	*SD (°C)*
Constant at 37°C	0-44	–0.22	0.21	0.02	0.08
Cooling	44-72	–0.38	0.32	–0.07	0.15
Constant at 27°C	72-129	–0.35	0.14	–0.07	0.08
Rewarming	129-160	–0.36	0.36	0.05	0.18
Constant at 37°C	160-275	–0.12	0.43	0.13	0.11
Full experiment	0-275	–0.38	0.43	0.04	0.14

tures were charted with 1°C precision at approximately 15 min intervals, providing a general reference for changes in body core temperature during the two-hour surgical procedure. Skin surface was measured with a thermistor embodied in the radiometer and deep brain temperature was monitored continuously with the radiometric sensor throughout the 120 minute surgical procedure, while the patient's whole body was cooled approximately 6°C and subsequently rewarmed. The calculated radiometric brain temperature was compared with the skin temperature under the sensor and with the nasopharyngeal and rectal core temperatures recorded manually by the anesthesiologist during the procedure.

Results

Figure 4 shows the HFSS-simulated receive pattern for the optimized antenna when placed on the experimental heterogeneous multilayer human head model. The receive pattern is shown for the center frequency of the radiometric band (1.35 GHz). Although there is a large signal (maximum in red) obtained from superficial scalp, it is clear that a significant portion of the microwave energy received by the antenna is derived from brain tissues inside the cranium. Note the minimal signal (in blue) collected from skull due to the low dielectric constant and dielectric loss of bone at microwave frequencies.

Figure 5 presents the radiometer response to serial 10°C changes in brain phantom temperature (37°C - 27°C - 37°C) while holding the superficial scalp region constant at 32°C. The radiometric signal (black curve) includes a 74 second delay caused by a 200 point median calculation applied in real time to smooth electromagnetic interference caused variations in the raw data. Although scalp temperature was maintained constant over the entire experiment, the deep penetrating radiometer sensor was able to track changes in brain phantom inside the skull precisely. The calculated radiometric equivalent brain temperatures and fiberoptic probe measured brain temperatures demonstrate a very high correlation ($r = 0.9979$ and $p < 0.001$) over this 4.6-hour experiment.

The accuracy and stability of the radiometric signal is shown in Figure 6, which presents the difference between the radiometer and fiberoptic measured temperatures of circulating brain phantom. The maximum difference during the entire experiment is 0.4°C. Table 1 presents a more detailed analysis of this temperature difference including relevant statistical parameters for each heating/cooling/steady state phase of the experiment. The difference is higher during times of rapidly changing temperature than during the three steady state periods.

Figure 7 shows the radiometric brain temperature of a one-year-old male patient along with measured rectal, nasopharyngeal, and skin temperatures during a two-hour surgical procedure. The brain temperature (solid black curve) was calculated from a median of 400 measured points (about five minutes of data) and thus lags the other core temperature measurements during the rapid cooling phase from 38 to 50 minutes into surgery. The data are plotted together with corresponding rectal and nasopharyngeal temperature measurements. Due to manual recording of core temperatures during pediatric cardiac anesthesia, rectal and nasopharyngeal temperatures may have up to 15 minutes uncertainty in timing relative to the precisely timed computer-acquired radiometric and skin data. Within this uncertainty, a loose correlation of falling and rising temperatures is seen between all core temperature measures. Notably, the nasopharyngeal and rectal measures exhibit a distinct time delay returning towards normothermia compared to the brain readings, producing a higher differ-

ential between brain and other core temperature surrogates during patient rewarming.

Throughout most of the two-hour surgical procedure recorded in Figure 7, the calculated radiometric brain temperature remained 1-2°C higher than other core temperatures, including skin. The calculated difference in core temperature measured in brain and rectum ($T_{brain} - T_{rectum}$) ranges from 0.4°C at their minimum values around 31°C to as high as 3.5°C at the peak brain temperature occurring 80 minutes into surgery. Similarly, the difference between the radiometric determination of brain temperature and the nasopharyngeal sensor ($T_{brain} - T_{naso}$) ranged from a minimum of 1°C at the beginning of surgery to a maximum of 4.5°C at the time of peak temperature in brain during reheating of the patient.

Discussion

There is extensive clinical evidence that measuring body core temperature accurately, during surgery and when returning patients quickly to the normothermic range following surgery has significant benefit to the patient in terms of speed of recovery and reduction of potential post-surgical complications. Currently this is of most benefit in managing patients recovering from hypothermic events such as cardiac surgery with temperature-regulated bypass perfusion, resuscitation of near drowning victims, or other severe hypothermia exposure. During these acute situations, the ability to provide rapid and accurate feedback of critically important core temperature as determined from the most vital tissue (brain) and abdominal organs would be invaluable to treating physicians. As is evident from Figure 7, the typical manual recording of patient's core temperature - with a precision of 1°C at approximately 15-minute intervals in surrogate sites like rectum or nasopharynx - produces an imprecise and time-delayed estimate of actual critical core temperature in brain.

The current effort introduces an entirely passive non-invasive thermometer capable of continuously monitoring core temperature directly within the brain. The measurement approach is based on the principle that thermal energy radiates from living tissue in proportion to temperature, with a significant amount of power emitted at microwave frequencies. This thermal radiation can be collected with a passive microwave receive antenna on the skin surface, amplified, filtered and quantified with a sensitive power detector. With appropriate electronics and software processing, the received power can be correlated directly with temperature of tissue located within the radiation field of the antenna. Such a measurement device is termed a microwave radiometer and is the subject of this study.

Attempts to use microwave radiometry for long-term monitoring of deep brain temperature have proven inadequate in the past due to: i) use of higher frequency (>2.5 GHz) radiometric bands and antennas that do not penetrate well, ii) lack of drift compensation for the radiometer electronics, and/or iii) not accounting for the correct percentage of signal coming from brain in different people caused by unique tissue geometry and impedance match [26-31].

The current experimental characterization of a novel microwave radiometer for deep tissue monitoring follows extensive development efforts of our group to optimize a lower frequency 1.1-1.6 GHz radiometer and deep penetrating, thick substrate, log spiral antennas [21-24]. With the HFSS-based simulation approach validated, a miniature 2.5 cm dia antenna was optimized for maximum sensitivity to thermal emissions from inside the human skull, with geometry determined from a CT scan of an adult human head. The antenna radiation patterns simulated for this realistic multilayer tissue load show that within the 1.1-1.6 GHz radiometric band up to 50% of the emitted energy captured by the surface antenna comes from tissue at depths of 1.4-4.5 cm (i.e. inside the skull). With knowledge of the skin surface temperature and a percentage of the total received signal emanating from brain, the equivalent brain temperature can be calculated from this single 500 MHz band radiometer.

The microwave antenna/radiometer sensor developed for this application allows direct core temperature measurements of critically important brain tissue from a small surface antenna. The sensing of thermal energy radiating from tissue by the antenna is entirely passive; there is no energy applied to the patient. The tests described in this study demonstrate that the radiometric sensor has high sensitivity to changes in brain temperature, and provides a stable signal over extended time periods since temperature references inside the radiometer sensor automatically compensate for drift in the gain of microwave electronics. The resulting accuracy is encouraging and appears to be within the range of currently used clinical core

temperature measurement devices [16] while providing much faster feedback of critically important brain temperature.

The maximum difference seen over the 4.6-hour phantom brain monitoring experiment was 0.4°C, which occurred during the rapid temperature changes when cooling (–0.57°C/min) and rewarming (0.62°C/min) the brain phantom. Although there was a 74s delay in measurements due to the moving median calculation window, the temperature changes in patients undergoing surgery are much slower (e.g. taking 20-30 minutes to heat or cool several degrees [25]). Thus, the transient temperature errors during rapid cooling and rewarming periods do not appear significant. In fact, the 74s delay in brain temperature calculation appears small compared to typical time delays of reading core temperature from remote sites like nasopharynx and rectum, as seen in Figure 7. Figure 5 shows cyclic variations of calculated radiometric temperature during the steady state periods with a maximum deviation of +0.27°C. The cyclic nature of these variations suggests that they may be the result of the pulsatile peristaltic pump-induced convection currents within the balloon, and thus correspond to actual small temperature variations in the brain phantom rather than electromagnetic noise.

It is important to note from the phantom study (Figure 5) that a significant portion of the radiometric measured temperature (in red) is derived from brain tissue inside the cranium, which was varied in temperature while holding the scalp (in blue) constant. It is true that the antenna receives a significant proportion of energy from tissues close to the surface, but the results of this study demonstrate our ability to read a radiometric signal directly proportional to temperature change in a region of brain under the antenna independent of the constant temperature scalp. Furthermore, the data demonstrate our ability to track changes in brain temperature over long time periods typical of open heart bypass surgery, enabling the physician to carefully monitor the patient's return to normothermic temperature quickly at the end of a long procedure.

As the initial step to introduce this technology into clinical use, this work reports one clinical case of monitoring deep brain temperature during a two-hour pediatric hypothermic cardiac surgery procedure. Although no gold standard measurement of brain temperature was available in this preliminary clinical case, an encouraging correlation is seen between falling and rising temperatures inside the brain with surrogate core temperature measures in the rectum and nasopharynx. While promising, a full clinical investigation is planned to confirm the utility of this new brain core temperature measurement device in surgical patients, by comparing the information from this non-invasive sensor with other core temperature monitoring approaches.

Conclusion

A non-invasive core temperature thermometer has been developed based on a single band 1.1-1.6 GHz microwave radiometer with progressive calibration technology. The accompanying radiometric sensor includes a dual-matched ultra-low noise pre-amplifier with internal temperature compensation and filtering, and a tapered log spiral antenna embedded in a lightweight and low profile 2.8 cm diameter by 1.5 cm high assembly. Experimental measurements were performed in a full-scale multilayer tissue model of the human head to confirm our ability to sense small temperature changes in deep brain, independent of the temperatures of overlying scalp and skull. This phantom study shows that a non-invasive microwave radiometer has the ability to track changes in brain temperature with an accuracy better than 0.5°C over long periods of time, as typical of open heart bypass surgery. Radiometric measurements of pediatric brain temperature during a two-hour surgical procedure demonstrate a loose correlation with core temperature measurements in rectum and nasopharynx, but appear to respond more quickly to changes in circulating blood temperature during patient rewarming. These data point to the clinical utility of this radiometric monitoring approach for rapid and safe non-invasive determination of critical brain temperature. This non-invasive assessment of volume-averaged brain core temperature should become a valuable tool to assist thermal management of patients undergoing surgery or recovery from hypothermic events and thus reduce complications from surgery.

Acknowledgements

The authors would like to recognize significant contributions from a diverse team of collaborators from the University of Tromso,

University of Rome Tor Vergata, University of L'Aquila, and University of Utah, as well as the encouragement and financial support from Doug Turnquist at Thermimage Inc. We would like to acknowledge the support of related technology development in NIH R21-DK092912 as well as software and hardware support from Ansys Corp, Agilent Technologies, National Instruments, and expert assistance from Don Pearce in the Duke University Machine Shop.

Funding for this research project was obtained from Thermimage Inc. (Salt Lake City, UT, USA) and related radiometer technology development was supported through NIH R21-DK092912.

References

1 Frank SM, Fleisher LA, Breslow MJ, et al. Perioperative maintenance of normothermia reduces the incidence of morbid cardiac events. A randomized clinical trial. JAMA. 1997; 277 (14): 1127-1134.
2 Kurz A, Sessler DI, Lenhardt R. Perioperative normothermia to reduce the incidence of surgical-wound infection and shorten hospitalization. N Engl J Med. 1996; 334 (19): 1209-1215.
3 Polderman KH. Mechanisms of action, physiological effects, and complications of hypothermia. Crit Care Med. 2009; 37 (7 Suppl): S186-S202.
4 Schmied H, Kurz A, Sessler DI, et al. Mild hypothermia increases blood loss and transfusion requirements during total hip arthroplasty. Lancet. 1996; 347 (8997): 289-292.
5 Winkler M, Akça O, Birkenberg B, et al. Aggressive warming reduces blood loss during hip arthroplasty. Anesth Analg. 2000; 91 (4): 978-984.
6 Rajagopalan S, Mascha E, Na J, et al. The effects of mild perioperative hypothermia on blood loss and transfusion requirement. Anesthesiology. 2008; 108 (1): 71-77.
7 Lenhardt R, Marker E, Goll V, et al. Mild intraoperative hypothermia prolongs postanesthetic recovery. Anesthesiology. 1997; 87 (6): 1318-1323.
8 Yan TD, Bannon PG, Bavaria J, et al. Consensus on hypothermia in aortic arch surgery. Ann Cardiothorac Surg. 2013; 2 (2): 163-168.
9 Roth JV. Some unanswered questions about temperature management. Anesth Analg. 2009; 109 (5): 1695-1699.
10 Hannenberg AA, Sessler DI. Improving perioperative temperature management. Anesth Analg. 2008; 107 (5): 1454-1457.
11 Lawson L, Bridges EJ, Ballou I, et al. Accuracy and precision of noninvasive temperature measurement in adult intensive care patients. Am J Crit Care. 2007; 16 (5): 485-496.
12 Pompei F, Pompei M. Non-invasive temporal artery thermometry: Physics, physiology, and clinical accuracy. Proc SPIE 5405: 61-67.
13 Moran JL, Peter JV, Solomon PJ, et al. Tympanic temperature measurements: Are they reliable in the critically ill? A clinical study of measures of agreement. Crit. Care Med. 2007; 35 (1): 155-164.
14 Pompei F. Misguided guidelines on noninvasive thermometry. Crit. Care Med. 2009; 37 (1): 383-384.
15 Haugk M, Stratil P, Sterz F, et al. Temperature monitored on the cuff surface of an endotracheal tube reflects body temperature. Crit Care Med. 2010; 38 (7): 1569-1573.
16 Sessler DI. Temperature monitoring and perioperative thermoregulation. Anesthesiology. 2008; 109 (2): 318-338.
17 McIlvoy L. Comparison of brain temperature to core temperature: a review of the literature. J Neurosci Nurs. 2004; 36 (1): 23-31.
18 Klemetsen O, Birkelund Y, Jacobsen SK, et al. Design of medical radiometer front-end for improved performance. Prog Electromagn Res B Pier B. 2011; 27: 289-306.
19 Hayman LA, Shukla V, Ly C, et al. Clinical and imaging anatomy of the scalp. J Comput Assist Tomogr. 2003; 27 (3): 454-459.
20 Gabriel S, Lau RW, Gabriel C. The dielectric properties of biological tissues III. Parametric models for the dielectric spectrum of tissues. Phys Med Biol. 1996; 41 (11): 2271-2293.
21 Arunachalam K, Maccarini P, De Luca V, et al. Modeling the detectability of vesicoureteral reflux using microwave radiometry. Phys Med Biol. 2010; 55 (18): 5417-5435.
22 Arunachalam K, Maccarini P, De Luca V, et al. Detection of vesicoureteral reflux using microwave radiometry-system characterization with tissue phantoms. IEEE Trans Biomed Eng. 2011; 58 (6): 1629-1636.
23 Stauffer P, Maccarini P, Arunachalam K, et al. Microwave radiometry for non-invasive detection of vesicoureteral reflux (VUR) following bladder warming. Proc SPIE. 2011; 7901: 79010V.
24 Birkelund Y, Klemetsen Ø, Jacobsen SK, et al. Vesicoureteral reflux in children: a phantom study of microwave heating and radiometric thermometry of pediatric bladder. IEEE Trans Biomed Eng. 2011; 58 (11): 3269-3278.
25 Sessler DI. Perioperative heat balance. Anesthesiology 2000; 92 (2): 578-596.
26 Bardati F, Iudicello S. Modeling the visibility of breast malignancy by a microwave radiometer. IEEE Trans Biomed Eng. 2008; 55 (1): 214-221.
27 Carr KL. Microwave radiometry: its importance to the detection of cancer. IEEE Trans Microw Theory Tech. 1989; 37 (12): 1862-1869.
28 Hand JW, Van Leeuwen GMJ, Mizushina S, et al. Monitoring of deep brain temperature in infants using multi-frequency microwave radiometry and thermal modelling. Phys Med Biol. 2001; 46 (7): 1885-1903.
29 Mizushina S, Ohba K, Abe K, et al. Recent trends in medical microwave radiometry. IEICE Trans Commun. 1995; E78B (6): 789-798.
30 Sterzer F. Microwave radiometers for non-invasive measurements of subsurface tissue temperatures. J Automedica. 1987; 8: 203-211.
31 Shaeffer J, El-Mahdi AM, Carr KL. Cancer detection studies using a 4.7 Gigahertz radiometer. Cancer Detect Prev. 1981; 4 (1-4): 571-578.

Paul R. Stauffer, MSEE, CCE
Professor and Director of Thermal Oncology Physics
Thomas Jefferson University
Radiation Oncology Dept.
Bodine Cancer Center Room G302A
111 S. 11th. St.
Philadelphia PA 19107
USA
Tel: 215-503-8825
E-mail: paul.stauffer@jeffersonhospital.org